


Article

Effect of Temperature on the Adhesion and Bactericidal Activities of Ag⁺-Doped BiVO₄ Ceramic Tiles

Ying Zhang ¹, Xuhuan Zhao ¹, Hao Wang ², Shiqi Fu ¹, Xiulong Lv ¹, Qian He ¹, Rui Liu ³, Fangying Ji ^{1,*} and Xuan Xu ^{1,*} 

¹ Key Laboratory of Three Gorges Reservoir Region's Eco-Environment, Ministry of Education, Chongqing University, Chongqing 400045, China; 201817131178@cqu.edu.cn (Y.Z.); z934098984@163.com (X.Z.); 201817131174@cqu.edu.cn (S.F.); xiulongallen@outlook.com (X.L.); 201817131139@cqu.edu.cn (Q.H.)

² Piesat Information Technology Co., Ltd., Beijing 100195, China; wanghao_jz@piesat.cn

³ Yunnan Ribo Testing Technology Co., Ltd., Kunming 650101, China; 237980491@163.com

* Correspondence: jfy@cqu.edu.cn (F.J.); xuxuan@cqu.edu.cn (X.X.)

Abstract: The aim of this research was to study the effect of temperature on the adhesion and disinfection activities of an Ag⁺-doped BiVO₄ (Ag⁺/BiVO₄) coating. Ag⁺/BiVO₄ was prepared by a sol-gel method, and spraying was used as the deposition method of coating. X-ray diffraction patterns showed that the monoclinic scheelite phase of the samples was unchanged by annealing at 450–650 °C. Scanning electron microscopy results showed that, at high temperatures, the particles melted and formed a dense coating, and the roughness of the coating decreased after initially increasing. The adhesion and disinfection activities were evaluated by ASTM D3359-08 and disinfection experiments. The results showed that the samples modified by silver had a good disinfection activity when annealed in the range of 450–650 °C. The adhesion increased upon increasing the annealing temperature. The sample annealed at 650 °C showed the best coating adhesion and completely killed *Escherichia coli*, *Staphylococcus aureus*, *Shigella*, and *Salmonella* after 2 h of visible-light irradiation.

Keywords: glazed ceramic tiles; disinfection activity; bismuth vanadate; coating adhesion



Citation: Zhang, Y.; Zhao, X.; Wang, H.; Fu, S.; Lv, X.; He, Q.; Liu, R.; Ji, F.; Xu, X. Effect of Temperature on the Adhesion and Bactericidal Activities of Ag⁺-Doped BiVO₄ Ceramic Tiles. *Inorganics* **2022**, *10*, 61. <https://doi.org/10.3390/inorganics10050061>

Academic Editor:
Alejandro Pérez-Larios

Received: 4 April 2022

Accepted: 1 May 2022

Published: 6 May 2022

Publisher's Note: MDPI stays neutral with regard to jurisdictional claims in published maps and institutional affiliations.



Copyright: © 2022 by the authors. Licensee MDPI, Basel, Switzerland. This article is an open access article distributed under the terms and conditions of the Creative Commons Attribution (CC BY) license (<https://creativecommons.org/licenses/by/4.0/>).

1. Introduction

The production of photocatalytic ceramic tiles with special functions, such as self-cleaning abilities, super-hydrophilicity, and antibacterial properties, has received attention in recent years [1]. TiO₂ is the most common photocatalyst due to its high chemical stability, good environmental friendliness, and low cost [2–4]. Unfortunately, TiO₂ is prone to an anatase-to-rutile transformation (ART) at high temperatures, significantly reducing its photocatalytic activity. At low temperatures (<950 °C), TiO₂ has extremely poor adhesion to ceramic tiles, which limits its immobilization [1,5]. BiVO₄ is non-toxic, environmentally friendly, and has excellent visible-light photocatalytic activity because the bandgap of monoclinic scheelite BiVO₄ is about 2.4 eV [6,7]. Unfortunately, it suffers from rapid recombination of photogenerated charge carriers, which greatly reduces its photocatalytic activity [8]. This can be overcome by doping or compounding it with other materials, such as Ag, BiOI, BiOCl, or CdS [9–11]. However, no studies have used BiVO₄ coatings on ceramic tiles.

Silver can form a Schottky barrier at the interface of photocatalytic materials, and the high conductivity of Ag can also improve the charge transfer rate of photocatalytic materials, which can improve electron-hole separation. In addition, silver has a better surface plasmon resonance (SPR) effect than other noble metals, which gives materials modified by silver a higher electron-hole separation efficiency and, thus, better photocatalytic activity [12,13]. Silver (Ag⁺) is also an excellent antibacterial agent [14].

Temperature has a significant effect on the photocatalytic activity and adhesion of coatings [1]. According to a previous study about BiVO₄, temperature affected the photocatalytic performance by changing the purity and particle size of BiVO₄. When the temperature is too high, grains will agglomerate, causing the particle size to increase. When the temperature is too low, other substances, such as Bi₄V₂O₁₁, can be found in materials that also decrease photocatalytic activity [15]. With regards to adhesion, current research has focused on TiO₂, and there is little research on the use of BiVO₄ coatings on ceramic tiles. Therefore, in this study, we studied the effect of temperature on the adhesion of coatings.

In this work, we prepared Ag⁺-doped BiVO₄ (Ag⁺/BiVO₄) by a sol-gel method and then immobilized it onto glazed ceramic tiles by spraying to prepare Ag/BiVO₄ functionalized ceramic tiles. Then, the effects of the annealing temperature on the phase, adhesion, morphology, roughness, and disinfection activities of the coatings were studied. This work may provide a material to replace TiO₂ in functionalized ceramic tiles.

2. Materials and Methods

2.1. Materials

All chemicals were used as received without further purification. Bismuth nitrate pentahydrate (Bi(NO₃)₃·5H₂O), ammonium vanadate (NH₄VO₃), and silver nitrate (AgNO₃) were all purchased from Chengdu Kelong Chemical Plant (AR purity, Chengdu, China). Glacial acetic acid (CH₃COOH), absolute ethanol (CH₃CH₂OH), and ammonium hydroxide (NH₄OH) were purchased from Chongqing Chuandong Chemical Co., Ltd. (AR purity, Chongqing, China). Nitric acid (HNO₃) was purchased from Chongqing Huihuang Chemical Co., Ltd. (AR purity, Chongqing, China). Glazed ceramic tiles were purchased from Guangdong Dongpeng Holdings Co., Ltd. (Guangdong, China) (The basic characteristics of the glazed ceramic tiles can be found in Supplementary Materials Table S1). All water was purified with a Millipore Ultra-purification System (Kun Shan Ultrasonic Instruments Co., Ltd., Kun Shan, China).

2.2. Ag⁺-Doped BiVO₄ Functionalized Ceramic Tiles Preparation

Ag⁺/BiVO₄ was prepared by a sol-gel method. The optimal Ag content was determined by disinfection experiments (as detailed in Supplementary Materials Figure S1). First, 0.728 g (Bi(NO₃)₃·5H₂O) and 0.046 g AgNO₃ were dissolved in 50 mL of 4 M HNO₃, and 0.175 g NH₄VO₃ was dissolved in 50 mL of 4 M NH₄OH. Then, the two solutions were mixed and magnetically stirred for 30 min to obtain a yellow solution. Ethanol (100 mL) was added to the yellow solution and heated at 70 °C with stirring for 60 min to obtain a yellow sol. Then, 50 mL deionized water and 5 mL 1 M CH₃COOH were added to the yellow sol and stirred for 30 min to obtain yellow sol-gel. The ceramic tiles were ultrasonically cleaned for 60 min and then sprayed with the sol-gel (the spray-coating procedure was adopted from K. Murugan et al. [16]). The tiles were then dried at 100 °C for 30 min and finally annealed at 450 °C, 550 °C, or 650 °C for 2 h to obtain Ag⁺/BiVO₄ functionalized ceramic tiles (named CSB, for ceramic-silver-bismuth vanadate) and unmodified BiVO₄ functionalized ceramic tiles (named CB, for ceramic-bismuth vanadate).

2.3. Disinfection Experiment

All instruments used in the disinfection experiments were sterilized in a steam sterilizer at 125 °C for 20 min.

The visible-light photocatalytic inactivation of *Escherichia coli* [ATCC25922], *Staphylococcus aureus* [ATCC6538], *Shigella* [CMCC (B) 51592], and *Salmonella* [CMCC (B) 50093] was conducted using a xenon lamp (1000 W; λ ≥ 420 nm) with a 420 nm cut-off filter. All bacteria were cultured in a nutrient agar medium for 16 h. The bacterial stock solution was prepared by dispersing bacteria in 0.9% sterile saline to obtain a concentration of 1 × 10⁸ CFU/mL (determined via a standard curve as detailed in the Supplementary Materials Figure S2). Next, 1 mL of the prepared bacterial solution was added to 99 mL of sterilized saline water, to which the functionalized ceramic tiles or uncoated ceramic tiles were added. A final sample group received

no further addition and served as a blank control group. Next, the prepared bacterial suspension was placed in a photoreactor under a xenon lamp for disinfection experiments at 25 °C. Samples were collected after irradiation for 5, 15, 30, 60, and 120 min. Three parallel samples were tested for each experiment.

After diluting the samples collected after disinfection to a certain concentration gradient according to continuous dilution, 0.1 mL of each sample was collected and evenly spread on nutrient agar for cultivation. Three gradient ranges were set for each sample, and four parallel samples were used for each gradient. The coated samples were placed in an incubator set to 37 °C and incubated upside-down for 24 h before counting.

2.4. Characterization

The crystal structure of the samples was determined by X-ray diffraction (XRD, X'Pert PRO, Rigaku, Japan). Cu-K α was the X-ray source ($\lambda = 0.15406$ nm), the power was 3 kW, and the 2θ scanning range was 10–80°. Ultraviolet-visible spectrophotometry (UV-Vis/DRS, UV3600, Shimadzu, Japan) was used to characterize the optical properties of the material. The surface roughness of the coatings was analyzed by atomic force microscopy (AFM, Dimension ICON, Bruker, Germany). The scanning area was 20 $\mu\text{m} \times 20 \mu\text{m}$. The morphology of the coatings was analyzed by field-emission scanning electron microscopy (SEM, S4800, Hitachi, Japan). Before tests, the surface of the sample was sputtered with gold. In addition, the Ag⁺ concentration in the disinfection experiments was measured by using inductively coupled plasma mass spectrometry (ICP-MS, PerkinElmer NexION 300X, USA).

The Standard Test Methods for Measuring Adhesion by Tape Test (D 3359-08) [17] was used to test the adhesion of the coatings. To verify the adhesion of the coatings to the glazed tiles, scratch tests (Micro-Combi tester, CSM, MCT, Switzerland) with a linearly increasing load (0.1 N to 30 N, scratch speed of 1 mm/min) were performed on the samples using a Rockwell indenter with a spherical tip (100 μm radius). Three scratches were created on each coating, with the minimum distance between two scratches set at 4 mm to achieve a representative average response over greater surfaces. The critical load L_{c1} (first crack) and L_{c2} (edge spallation) were determined by optical microscopy.

3. Results and Discussion

3.1. Phase, Chemical and Optical Characterization

Figure 1 shows the XRD patterns of BiVO₄ and Ag/BiVO₄ coatings annealed at 450 °C, 550 °C, and 650 °C.

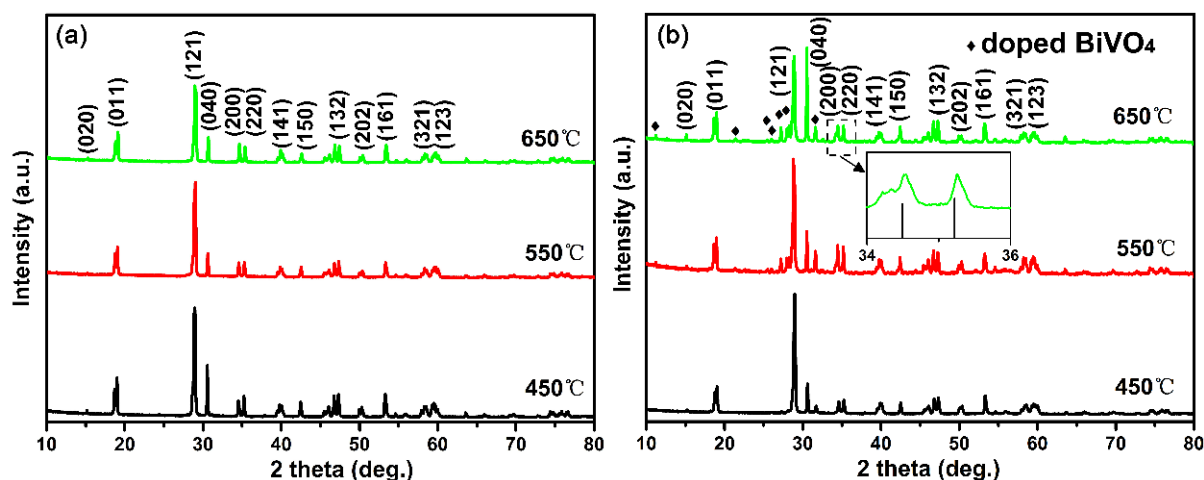


Figure 1. (a) XRD patterns of BiVO₄ and (b) Ag/BiVO₄ coatings obtained at different annealed temperatures.

Comparing BiVO₄ and Ag/BiVO₄ coatings with the corresponding standard diffraction data (JCPDS 14-0688) revealed that BiVO₄ existed as monoclinic scheelite. The diffrac-

tion peaks at 15.14° , 18.98° , 28.94° , 30.54° , 34.49° , 37.86° , 39.54° , and 42.33° correspond to the (020), (011), (121), (040), (200), (220), (141) and (150) facets of BiVO_4 , and no additional peaks were observed. These results indicate that BiVO_4 and Ag/BiVO_4 phases were unaffected by temperature within the range of $550\text{--}650^\circ\text{C}$, revealing their good thermal stability. Figure 1b shows that major characteristic peaks at 11.3° , 28.0° , 21.5° , 25.5° , 26.0° , 28.3° , and 31.70° were observed, which were due to the formation of hybrid metal oxides on the surface of the material. [18,19]. These findings implied that sliver and temperature did not change the lattice structure of BiVO_4 . Interestingly, Figure 1b shows that when the temperature increased to 650°C , the XRD peaks of Ag/BiVO_4 shifted slightly to the right due to the smaller ionic radius of Bi^{3+} (103 pm) than Ag^+ (115 pm), showing that Ag^+ replaced Bi^{3+} during the preparation process [20]. Upon increasing the temperature, the intensities of the peaks representing the (040) and (020) planes of Ag/BiVO_4 increased significantly because a high temperature led to the rapid decomposition of vanadate and an increase in the pH, which promoted the formation of BiVO_4 [21].

Figure S3 shows the XPS spectra of BiVO_4 and Ag/BiVO_4 . Early studies about Ag , Ag_2O , and AgO showed that the order of binding energy of $\text{Ag}3d_{5/2}$ was Ag (368.2 eV) > Ag_2O (367.8 eV) > AgO (367.4 eV) [19]. Therefore, Ag was in the +1 valence state, showing that the composite material was $\text{Ag}^+/\text{BiVO}_4$. Figure S3c is the characteristic peak of oxygen. It can be seen that there were two diffraction peaks of O at binding energies of 529.8 eV and 531.9 eV, indicating that at least two kinds of oxygen are present. The first peak belongs to completely oxidized oxygen ions, and the latter peak corresponds to external OH groups or water molecules adsorbed on the surface of the single-bond sample. Figure S2d shows that V produced a set of double peaks at 516.5 eV and 523.8 eV, which were attributed to $\text{V}2p_{5/2}$ and $\text{V}2p_{3/2}$, respectively. Figure S3e shows that Bi produced peaks at 158.9 eV and 164.2 eV, which were attributed to $\text{Bi}4f_{7/2}$ and $\text{Bi}4f_{5/2}$ [9,18].

The UV-Vis spectra of BiVO_4 and Ag/BiVO_4 are shown in Figure S4a. The absorption edge of pure BiVO_4 is at about 527 nm, which is slightly higher than the reported absorption edge (504 nm).

This may be due to the sample's large particle size and surface defects. Compared with BiVO_4 , the absorption capacity of Ag/BiVO_4 increased to 500–850 nm due to the charge transfer between Ag and BiVO_4 [22]. This indicates that Ag/BiVO_4 has better optical properties than pure BiVO_4 . The bandgap of a semiconductor is another important factor that determines its photocatalytic performance; therefore, we also calculated the bandgap energy (E_g) of BiVO_4 and Ag/BiVO_4 according to the reported equation [23]:

$$\alpha = A(h\nu - E_g)^{n/2}/h\nu \quad (1)$$

where α , h , ν , A , and E_g are the absorption coefficient, Planck's constant, incident light frequency, constant, and bandgap energy, respectively. n depends on the characteristics of the optical transition of the semiconductors, where $n = 1$ for direct and $n = 4$ for indirect bandgap semiconductors. BiVO_4 is a typical direct bandgap semiconductor. From the $(\alpha h\nu)^2$ versus E_g plot shown in Figure S4b, the bandgaps of BiVO_4 and Ag/BiVO_4 were 2.35 eV and 2.15 eV, respectively. The bandgap of Ag/BiVO_4 was smaller, so all samples should have a bandgap suitable for sterilization under visible light irradiation [24].

3.2. Adhesion of Coating on Ceramic Tiles

Adhesion is the most critical variable determining whether a photocatalytic coating can be applied to ceramic tiles, but few studies in the literature have evaluated this [16,25–27]. In this study, adhesion tests were performed according to ASTM D 3359-08 [17], and scratch tests were also performed. The results were classified into six grades: 0B, 1B, 2B, 3B, 4B, and 5B. The adhesion of these grades successively increased.

Table 1 shows the coating adhesion test results of functionalized ceramic tiles annealed at different temperatures. Both BiVO_4 and Ag/BiVO_4 coatings achieved 3B at 450°C . The coating was greatly affected by temperature, showing increasing adhesion upon increasing the temperature. At 650°C , the coating adhesion was the best. In addition, the Ag species

increased the photocatalytic coating's adhesion to the ceramic tiles, indicating that Ag species helped immobilize the photocatalytic materials on the surface of ceramic tiles, but their influence was small.

Table 1. The tape test results of functionalized ceramic tiles were sintered at different temperatures.

Sample	Temperature/°C	Percent of Area Removed			Classification
		1st/%	2nd/%	3rd/%	
CB	450	5	5	10	3B
CSB		5	10	3	3B
CB	550	3	2	6	3B
CSB		0	1	1	4B
CB	650	0	0	0	5B
CSB		0	0	0	5B

In addition, scratch tests with a linearly increasing load were performed on the samples to characterize the adhesion of the coated surface (the). In Table 2, the first (coating failure) and second (coating detachment) critical load values are reported. Compared with the reported results of titanium dioxide [26,27], Ag/BiVO₄-functionalized ceramic tiles annealed at 650 °C have good adhesion. The scratch track appeared at a higher load with BiVO₄ and Ag/BiVO₄, as shown in the optical images in Figure 2. Obviously, the CSB samples presented higher critical loads because they failed at 8.0 N and were removed at 18.8 N (Table 2, Figure S5). This phenomenon was explained using SEM data.

Table 2. First critical load (L_{c1}) and second critical load (L_{c2}) of the samples.

Sample	L_{c1} (N)	L_{c2} (N)
CB	2.1 ± 0.3	17.0 ± 0.5
CSB	8.0 ± 0.9	18.8 ± 1

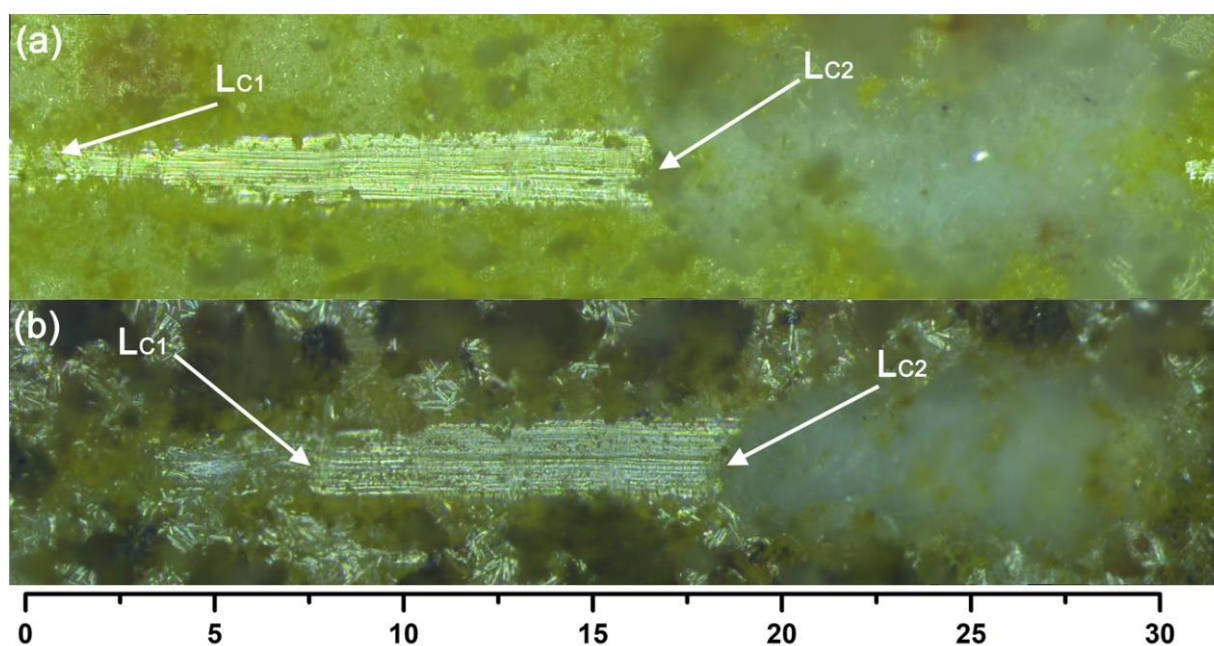


Figure 2. Optical images of the samples (annealed at 650 °C) after the scratch tests. (a) BiVO₄ photocatalytic ceramic tiles; (b) Ag/BiVO₄ photocatalytic ceramic tiles.

3.3. Coating Microstructure and Morphology

SEM was used to investigate the adhesion and morphology of the coatings obtained at different temperatures. Figures 3–5 and S6 show the SEM images of samples obtained at different annealing temperatures. As shown in Figures 4 and 5, there were large voids between the photocatalyst particles on the surface of the coating, which led to poor adhesion of the coating, causing the photocatalyst particles to agglomerate. At 550 °C (Figure 4), the voids between the photocatalyst particles on the surface of the ceramic tile decreased. This phenomenon was more evident in BiVO₄ functionalized ceramic tiles, while a small amount of photocatalyst melted and fused to form a dense coating on the surface of CSB. When the temperature increased to 650 °C (Figure 5), the photocatalytic materials immobilized on the surface of CB agglomerated into larger particles. This phenomenon was more obvious in CSB, in which the particles melted to form a dense coating structure, giving the coating on the surface of CSB the best adhesion. In addition to the temperature, silver significantly affected the morphology of the coating. Ag⁺ promoted the mutual melting of BiVO₄ particles, so the voids between catalyst particles on the surface of CSB were much smaller, which improved the adhesion. Figure S6 shows that the thickness of the Ag/BiVO₄ coating annealed at 650 °C was 17.64 μm, which was attributed to the large particle size.

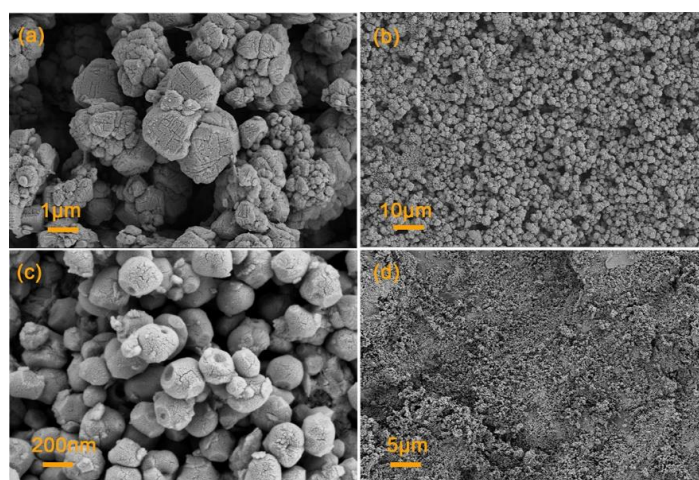


Figure 3. SEM images of (a,b) BiVO₄ and (c,d) Ag/BiVO₄ functionalized ceramic tiles obtained at 450 °C.

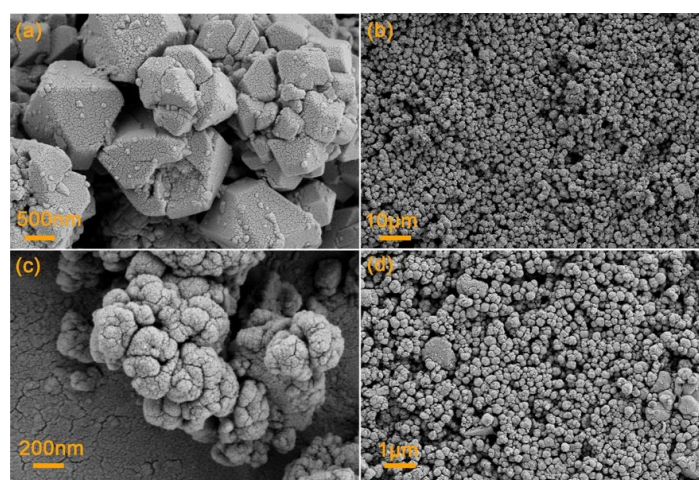


Figure 4. SEM images of (a,b) BiVO₄ and (c,d) Ag/BiVO₄ functionalized ceramic tiles obtained at 550 °C.

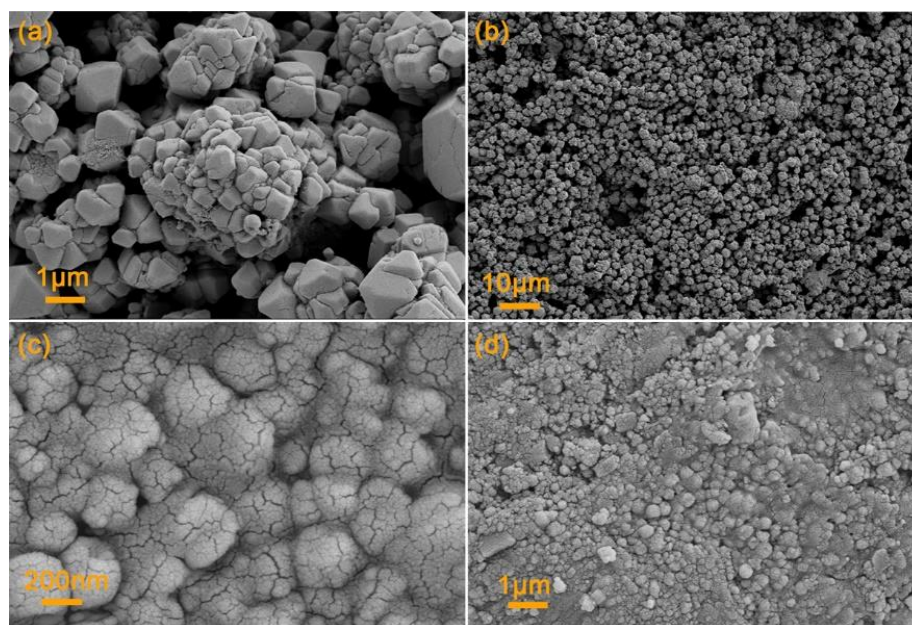


Figure 5. SEM images of (a,b) BiVO_4 and (c,d) Ag/BiVO_4 functionalized ceramic tiles obtained at $650\text{ }^\circ\text{C}$.

Figures S7–S9 show the AFM images of the samples obtained at different temperatures. At $450\text{ }^\circ\text{C}$, the roughness (estimated by arithmetical mean deviation of the profile (R_a)) of CB and CSB was 70.2 nm and 141 nm , respectively. When the temperature increased to $550\text{ }^\circ\text{C}$, the roughness of the two samples increased to 117 nm and 162 nm , respectively. When the temperature increased to $650\text{ }^\circ\text{C}$, the roughness decreased to 100 nm and 117 nm , respectively. Studies have shown that the agglomeration and particle size of photocatalytic materials affect their parameters. When a material agglomerates or melts into larger particles, the roughness of the coating will increase [28]. The SEM results show that when the temperature increased from $450\text{ }^\circ\text{C}$ to $550\text{ }^\circ\text{C}$, the photocatalytic particles agglomerated, which increased the surface roughness of the coated ceramic tiles. As the temperature increased to $650\text{ }^\circ\text{C}$, the roughness decreased. The reason is that the photocatalytic particles on the surface of the ceramic tiles melted at high temperatures, and the voids between the materials gradually decreased, which decreased the roughness of the coating. Compared with CB, the CSB coating had a much higher roughness for the hybrid metal oxides on the surface of BiVO_4 (determined from SEM, as detailed in Figures S10 and S11). Studies have shown that surfaces with a higher roughness have a greater surface area, which increases the photocatalytic reaction rate [29]. Therefore, CSB displayed higher disinfection efficiency.

3.4. Disinfection Results

The sterilization effects of the samples at different temperatures were evaluated by disinfection experiments, and the results are shown in Figure 6a. The bacterial concentration using glazed ceramic tiles was almost unchanged, indicating that unmodified ceramic tiles cannot kill bacteria. Upon increasing the temperature, the disinfection efficiency of CB and CSB decreased. The reason can be attributed to particle melting and agglomeration at high temperatures, which increased the particle size and decreased the available surface area, so the bactericidal effect was worse. This increased the particle size of the material, which decreased its disinfection efficiency [30,31]. Compared with CB, CSB had a higher disinfection efficiency, and the CSB annealed within the range $450\text{--}650\text{ }^\circ\text{C}$ killed 100% of bacteria after disinfection under visible light irradiation for 2 h.

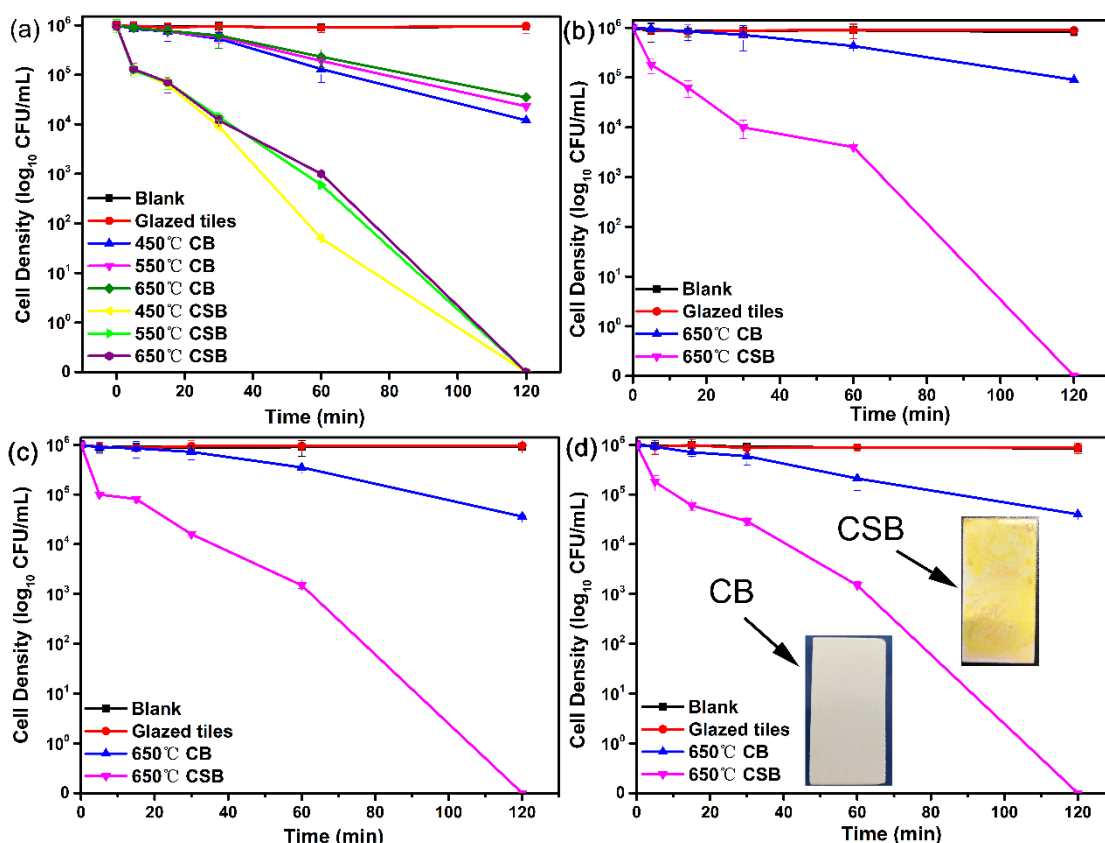


Figure 6. *Escherichia coli* disinfection efficiency of BiVO_4 and Ag/BiVO_4 ceramic tiles annealed at different temperatures (a) and ceramic tiles disinfection efficiency under different bacterial species. (b) *Staphylococcus aureus*, (c) *Salmonella*, and (d) *Shigella* (bacterial suspension concentration: 1×10^6 CFU/mL; common anions: 0.9% Cl^-).

To illustrate that the functionalized ceramic tiles have good application prospects, the tiles annealed at 650°C were selected for disinfection experiments using different bacteria species, and the results are shown in Figure 6a–d. The experimental results confirmed that CSB had a high disinfection efficiency against gram-negative bacteria such as *E. coli* and gram-positive bacteria such as *Staphylococcus aureus*, *Shigella*, and *Salmonella*. In addition, CSB showed a high disinfection efficiency, and it completely killed four common pathogenic bacteria after visible light irradiation for 2 h. Compared with TiO_2 -coated ceramic tiles [27,32], $\text{Ag}^+/\text{BiVO}_4$ -functionalized ceramic tiles annealed at 650°C displayed the highest disinfection efficiency. In addition, the concentrations of released Ag^+ (Figure S12) remained under $100\ \mu\text{g}/\text{L}$. A previous study [33] showed that the inactivation effect of $100\ \mu\text{g}/\text{L}$ Ag^+ was only $0.9\ \log\ \text{CFU}/\text{mL}$ in 3 h; therefore, the contribution of Ag^+ from $\text{Ag}^+/\text{BiVO}_4$ functionalized ceramic tiles was negligible.

4. Conclusions

BiVO_4 and Ag/BiVO_4 -coated ceramic tiles were prepared using a sol–gel and spraying method. A disinfection experiment and subsequent characterization investigated the effect of temperature. It was found that temperature had little effect on the phases of BiVO_4 and Ag/BiVO_4 , but it greatly influenced the adhesion and disinfection activities of the coatings. This was attributed to the melting and agglomeration of photocatalytic particles at 550°C , which then formed a dense coating structure at 650°C . Moreover, the experimental results demonstrated that the Ag/BiVO_4 -functionalized ceramic tiles annealed at 650°C displayed the best adhesion and killed various bacteria after 2 h of visible-light irradiation. Therefore, Ag/BiVO_4 -functionalized ceramic tiles are promising candidates for practical applications.

Supplementary Materials: The following supporting information can be downloaded at: <https://www.mdpi.com/article/10.3390/inorganics10050061/s1>, Figure S1: The effect of Ag dosage on the sterilization effect of Ag/BiVO₄ obtained at 450 °C (bacterial suspension concentration: 1 × 10⁶ CFU/mL; bacterial species: *Escherichia coli*; common anions: 0.9% Cl⁻); Figure S2: Standard curve of bacteria suspension concentration vs. absorbance (wavelength: 600 nm); Figure S3: XPS spectra of BiVO₄ and Ag/BiVO₄ powder (prepared temperature: 450 °C): (a) Full-scan spectra of BiVO₄ and Ag/BiVO₄; (b–e) peak positions of Ag, O, V, and Bi species; Figure S4: (a) UV-Vis spectra of samples prepared at 450 °C; (b) band gap widths of the samples prepared at 450 °C; Figure S5: *Escherichia* disinfection efficiency of Ag/BiVO₄ ceramic tiles after scratch tests (bacterial suspension concentration: 1 × 10⁶ CFU/mL; common anions: 0.9% Cl⁻); Figure S6: SEM cross-section image of Ag/BiVO₄ coating obtained at 650 °C; Figure S7: AFM images of (a–b) BiVO₄ and (c–d) Ag/BiVO₄-functionalized ceramic tiles annealed at 450 °C; Figure S8: AFM images of (a–b) BiVO₄ and (c–d) Ag/BiVO₄-functionalized ceramic tiles annealed at 550 °C; Figure S9: AFM images of (a–b) BiVO₄ and (c–d) Ag/BiVO₄-functionalized ceramic tiles annealed at 650 °C; Figure S10: (a–c) SEM images of BiVO₄ and (d–f) Ag/BiVO₄ powders at 450 °C; Figure S11: Grain size distribution of BiVO₄ and (a) Ag/BiVO₄ (b) powder obtained at 450 °C; Figure S12: Concentration of Ag⁺ released from Ag/BiVO₄-functionalized ceramic tiles annealed at 650 °C; Table S1: The basic characteristics of glazed ceramic tiles (model number: 630ELN52005-A).

Author Contributions: Y.Z.: conceptualization; data curation; investigation; methodology; resources; writing—original draft; writing—review and editing. X.Z., H.W., S.F., X.L., R.L. and Q.H.: writing—review and editing; project administration; supervision. F.J. and X.X.: resources; writing—review and editing. All authors have read and agreed to the published version of the manuscript.

Funding: This research was funded by the National Key Research and Development Program (2018YFD1100501).

Institutional Review Board Statement: Not applicable.

Informed Consent Statement: Not applicable.

Conflicts of Interest: The authors declare that they have no known competing financial interests or personal relationships that could have appeared to influence the work reported in this paper.

References

1. da Silva, A.L.; Dondi, M.; Raimondo, M.; Hotza, D. Photocatalytic ceramic tiles: Challenges and technological solutions. *J. Eur. Ceram. Soc.* **2018**, *38*, 1002–1017. [[CrossRef](#)]
2. da Silva, A.L.; Muche, D.N.F.; Dey, S.; Hotza, D.; Castro, R.H.R. Photocatalytic Nb₂O₅-doped TiO₂ nanoparticles for glazed ceramic tiles. *Ceram. Int.* **2016**, *42*, 5113–5122. [[CrossRef](#)]
3. Fujishima, A.; Zhang, X.; Tryk, D.A. TiO₂ photocatalysis and related surface phenomena. *Surf. Sci. Rep.* **2008**, *63*, 515–582. [[CrossRef](#)]
4. Zhang, H.; Banfield, J.F. Structural Characteristics and Mechanical and Thermodynamic Properties of Nanocrystalline TiO₂. *Chem. Rev.* **2014**, *114*, 9613–9644. [[CrossRef](#)] [[PubMed](#)]
5. Seabra, M.P.; Pires, R.R.; Labrincha, J.A. Ceramic tiles for photodegradation of Orange II solutions. *Chem. Eng. J.* **2011**, *171*, 692–702. [[CrossRef](#)]
6. Ye, L.; Su, Y.; Jin, X.; Xie, H.; Zhang, C. Recent advances in BiOX (X = Cl, Br and I) photocatalysts: Synthesis, modification, facet effects and mechanisms. *Environ. Sci. Nano* **2014**, *1*, 90–112. [[CrossRef](#)]
7. Qu, Z.; Liu, P.; Yang, X.; Wang, F.; Zhang, W.; Fei, C. Microstructure and Characteristic of BiVO₄ Prepared under Different pH Values: Photocatalytic Efficiency and Antibacterial Activity. *Materials* **2016**, *9*, 129. [[CrossRef](#)]
8. Zhao, D.; Wang, W.; Sun, Y.; Fan, Z.; Du, M.; Zhang, Q.; Ji, F.; Xu, X. One-step synthesis of composite material MWCNT@BiVO₄ and its photocatalytic activity. *RSC Adv.* **2017**, *7*, 33671–33679. [[CrossRef](#)]
9. Regmi, C.; Dhakal, D.; Lee, S.W. Visible-light-induced Ag/BiVO₄ semiconductor with enhanced photocatalytic and antibacterial performance. *Nanotechnology* **2018**, *29*, 064001. [[CrossRef](#)]
10. Guo, R.; Yan, A.; Xu, J.; Xu, B.; Li, T.; Liu, X.; Yi, T.; Luo, S. Effects of morphology on the visible-light-driven photocatalytic and bactericidal properties of BiVO₄/CdS heterojunctions: A discussion on photocatalysis mechanism. *J. Alloy. Compd.* **2020**, *817*, 153246. [[CrossRef](#)]
11. He, Z.; Shi, Y.; Gao, C.; Wen, L.; Chen, J.; Song, S. BiOCl/BiVO₄ p–n Heterojunction with Enhanced Photocatalytic Activity under Visible-Light Irradiation. *J. Phys. Chem. C* **2013**, *118*, 389–398. [[CrossRef](#)]
12. Xu, X.; Yan, Q.; Gu, X.; Luo, Y. The preparation and photocatalytic performance of BiOCl@Ag, a visible-light responsive catalyst. *J. Mater. Sci. Mater. Electron.* **2019**, *30*, 8892–8902. [[CrossRef](#)]

13. Di, J.; Xia, J.; Ji, M.; Wang, B.; Yin, S.; Huang, Y.; Chen, Z.; Li, H. New insight of Ag quantum dots with the improved molecular oxygen activation ability for photocatalytic applications. *Appl. Catal. B Environ.* **2016**, *188*, 376–387. [[CrossRef](#)]
14. Simončič, B.; Klemenčič, D. Preparation and performance of silver as an antimicrobial agent for textiles: A review. *Text. Res. J.* **2015**, *86*, 210–223. [[CrossRef](#)]
15. Shen, Y.; Wang, X.; Zuo, G.; Li, F.; Meng, Y. Influence of Heat Treatment on Photocatalytic Performance of BiVO₄ Synthesized by Hydrothermal Method. *High Temp. Mater. Processes* **2016**, *35*, 853–856. [[CrossRef](#)]
16. Murugan, K.; Subasri, R.; Rao, T.N.; Gandhi, A.S.; Murty, B.S. Synthesis, characterization and demonstration of self-cleaning TiO₂ coatings on glass and glazed ceramic tiles. *Prog. Org. Coat.* **2013**, *76*, 1756–1760. [[CrossRef](#)]
17. ASTM D3359-08; Standard Test Methods for Measuring Adhesion by Tape Test. ASTM International: West Conshohocken, PA, USA, 2008.
18. Wang, K.; Liang, L.; Liu, H.; Xie, X.; Hao, Q.; Liu, C. Facile synthesis of hollow and porous Ag⁺/Ag/BiVO₄ composite fibers with enhanced visible-light photocatalytic performance. *Mater. Lett.* **2015**, *161*, 336–339. [[CrossRef](#)]
19. Zhou, B.; Zhao, X.; Liu, H.; Qu, J.; Huang, C.P. Synthesis of visible-light sensitive M-BiVO₄ (M=Ag, Co, and Ni) for the photocatalytic degradation of organic pollutants. *Sep. Purif. Technol.* **2011**, *77*, 275–282. [[CrossRef](#)]
20. Shan, L.; Liu, Y.; Ma, C.; Dong, L.; Liu, L.; Wu, Z. Enhanced Photocatalytic Performance in Ag⁺-Induced BiVO₄/β-Bi₂O₃ Heterojunctions. *Eur. J. Inorg. Chem.* **2016**, *2016*, 232–239. [[CrossRef](#)]
21. Thalluri, S.M.; Hussain, M.; Saracco, G.; Barber, J.; Russo, N. Green-Synthesized BiVO₄ Oriented along {040} Facets for Visible-Light-Driven Ethylene Degradation. *Ind. Eng. Chem. Res.* **2014**, *53*, 2640–2646. [[CrossRef](#)]
22. Sayama, K.; Nomura, A.; Arai, T.; Sugita, T.; Abe, R.; Yanagida, M.; Oi, T.; Iwasaki, Y.; Abe, Y.; Sugihara, H. Photoelectrochemical Decomposition of Water into H₂ and O₂ on Porous BiVO₄ Thin-Film Electrodes under Visible Light and Significant Effect of Ag Ion Treatment. *J. Phys. Chem. B* **2006**, *110*, 11352–11360. [[CrossRef](#)] [[PubMed](#)]
23. Yan, M.; Wu, Y.; Yan, Y.; Yan, X.; Zhu, F.; Hua, Y.; Shi, W. Synthesis and Characterization of Novel BiVO₄/Ag₃VO₄ Heterojunction with Enhanced Visible-Light-Driven Photocatalytic Degradation of Dyes. *ACS Sustain. Chem. Eng.* **2016**, *4*, 757–766. [[CrossRef](#)]
24. Zeng, X.; Lan, S.; Lo, I.M.C. Rapid disinfection of E. coli by a ternary BiVO₄/Ag/g-C₃N₄ composite under visible light: Photocatalytic mechanism and performance investigation in authentic sewage. *Environ. Sci. Nano* **2019**, *6*, 610–623. [[CrossRef](#)]
25. Raimondo, M.; Guarini, G.; Zanelli, C.; Marani, F.; Fossa, L.; Dondi, M. Printing nano TiO₂ on large-sized building materials: Technologies, surface modifications and functional behaviour. *Ceram. Int.* **2012**, *38*, 4685–4693. [[CrossRef](#)]
26. Bondioli, F.; Taurino, R.; Ferrari, A.M. Functionalization of ceramic tile surface by sol-gel technique. *J. Colloid Interface Sci.* **2009**, *334*, 195–201. [[CrossRef](#)]
27. de Niederhäusern, S.; Bondi, M.; Bondioli, F. Self-Cleaning and Antibacteric Ceramic Tile Surface. *Int. J. Appl. Ceram. Technol.* **2013**, *10*, 949–956. [[CrossRef](#)]
28. Kete, M.; Pavlica, E.; Fresno, F.; Bratina, G.; Stangar, U.L. Highly active photocatalytic coatings prepared by a low-temperature method. *Environ. Sci. Pollut. Res. Int.* **2014**, *21*, 11238–11249. [[CrossRef](#)]
29. Mellott, N.P.; Durucan, C.; Pantano, C.G.; Guglielmi, M. Commercial and laboratory prepared titanium dioxide thin films for self-cleaning glasses: Photocatalytic performance and chemical durability. *Thin Solid Film.* **2006**, *502*, 112–120. [[CrossRef](#)]
30. Li, Y.; Sun, H.; Wang, N.; Fang, W.; Li, Z. Effects of pH and temperature on photocatalytic activity of PbTiO₃ synthesized by hydrothermal method. *Solid State Sci.* **2014**, *37*, 18–22. [[CrossRef](#)]
31. Qi, Y.; Wang, M.; Zhang, Y.; Zhu, T. Effect of calcination temperature on the structure and photocatalytic performance of BiVO₄ prepared via an improved solution combustion method. *Micro Nano Lett.* **2018**, *13*, 1017–1020. [[CrossRef](#)]
32. Sun, S.Q.; Sun, B.; Zhang, W.; Wang, D. Preparation and antibacterial activity of Ag-TiO₂ composite film by liquid phase deposition (LPD) method. *Bull. Mater. Sci.* **2008**, *31*, 61–66. [[CrossRef](#)]
33. Jin, Y.; Dai, Z.; Liu, F.; Kim, H.; Tong, M.; Hou, Y. Bactericidal mechanisms of Ag₂O/TNBs under both dark and light conditions. *Water Res.* **2013**, *47*, 1837–1847. [[CrossRef](#)] [[PubMed](#)]